



OPEN ACCESS

EDITED BY

Sumit Kumar Hira,
University of Burdwan, India

REVIEWED BY

Bilash Chatterjee,
Indian Institute of Chemical Biology (CSIR),
India
Subhadip Pati,
University of North Carolina at Chapel Hill,
United States

*CORRESPONDENCE

Susheela Tridandapani
✉ tridandapani.2@osu.edu
Jonathan P. Butchar
✉ butchar.2@osu.edu

†These authors have contributed
equally to this work and share
last authorship

RECEIVED 29 March 2024

ACCEPTED 21 May 2024

PUBLISHED 11 June 2024

CITATION

Merchand-Reyes G, Bull MF, Santhanam R,
Valencia-Pena ML, Murugesan RA,
Chordia A, Mo X-M, Robledo-Avila FH,
Ruiz-Rosado JDD, Carson III WE, Byrd JC,
Woyach JA, Tridandapani S and Butchar JP
(2024) NOD2 activation enhances
macrophage Fcγ receptor function and may
increase the efficacy of antibody therapy.
Front. Immunol. 15:1409333.
doi: 10.3389/fimmu.2024.1409333

COPYRIGHT

© 2024 Merchand-Reyes, Bull, Santhanam,
Valencia-Pena, Murugesan, Chordia, Mo,
Robledo-Avila, Ruiz-Rosado, Carson, Byrd,
Woyach, Tridandapani and Butchar. This is an
open-access article distributed under the terms
of the [Creative Commons Attribution License
\(CC BY\)](https://creativecommons.org/licenses/by/4.0/). The use, distribution or reproduction
in other forums is permitted, provided the
original author(s) and the copyright owner(s)
are credited and that the original publication
in this journal is cited, in accordance with
accepted academic practice. No use,
distribution or reproduction is permitted
which does not comply with these terms.

NOD2 activation enhances macrophage Fcγ receptor function and may increase the efficacy of antibody therapy

Giovanna Merchand-Reyes¹, Mikayla F. Bull²,
Ramasamy Santhanam¹, Maria L. Valencia-Pena¹,
Rakesh A. Murugesan², Aadesh Chordia², Xiaokui-Molly Mo³,
Frank H. Robledo-Avila⁴, Juan De Dios Ruiz-Rosado^{5,6},
William Edgar Carson III⁷, John C. Byrd⁸, Jennifer A. Woyach¹,
Susheela Tridandapani^{1*†} and Jonathan P. Butchar^{1*†}

¹Division of Hematology, Department of Internal Medicine, College of Medicine, The Ohio State University, Columbus, OH, United States, ²College of Medicine, The Ohio State University, Columbus, OH, United States, ³Department of Biomedical Informatics, The Ohio State University, Columbus, OH, United States, ⁴Center for Microbial Pathogenesis, Abigail Wexner Research Institute, Nationwide Children's Hospital, Columbus, OH, United States, ⁵Kidney and Urinary Tract Center, Abigail Wexner Research Institute, Nationwide Children's Hospital, Columbus, OH, United States, ⁶Division of Pediatric Nephrology and Hypertension, Nationwide Children's Hospital, Columbus, OH, United States, ⁷Department of Surgery, The Ohio State University, Columbus, OH, United States, ⁸Department of Internal Medicine, College of Medicine, University of Cincinnati, Cincinnati, OH, United States

Introduction: Therapeutic antibodies have become a major strategy to treat oncologic diseases. For chronic lymphocytic leukemia, antibodies against CD20 are used to target and elicit cytotoxic responses against malignant B cells. However, efficacy is often compromised due to a suppressive microenvironment that interferes with cellular immune responses. To overcome this suppression, agonists of pattern recognition receptors have been studied which promote direct cytotoxicity or elicit anti-tumoral immune responses. NOD2 is an intracellular pattern recognition receptor that participates in the detection of peptidoglycan, a key component of bacterial cell walls. This detection then mediates the activation of multiple signaling pathways in myeloid cells. Although several NOD2 agonists are being used worldwide, the potential benefit of these agents in the context of antibody therapy has not been explored.

Methods: Primary cells from healthy-donor volunteers (PBMCs, monocytes) or CLL patients (monocytes) were treated with versus without the NOD2 agonist L18-MDP, then antibody-mediated responses were assessed. In vivo, the Eμ-TCL1 mouse model of CLL was used to test the effects of L18-MDP treatment alone and in combination with anti-CD20 antibody.

Results: Treatment of peripheral blood mononuclear cells with L18-MDP led to activation of monocytes from both healthy donors and CLL patients. In addition, there was an upregulation of activating FcγR in monocytes and a subsequent increase in antibody-mediated phagocytosis. This effect required the NF-κB and p38 signaling pathways. Treatment with L18-MDP plus anti-CD20 antibody in the

E μ -TCL model of CLL led to a significant reduction of CLL load, as well as to phenotypic changes in splenic monocytes and macrophages.

Conclusions: Taken together, these results suggest that NOD2 agonists help overturn the suppression of myeloid cells, and may improve the efficacy of antibody therapy for CLL.

KEYWORDS

NOD2 agonists, monocytes, chronic lymphocytic leukemia, antibody-mediated responses, pre-clinical model

1 Introduction

Antibody therapy has been successfully used to treat oncologic diseases for more than 20 years. Rituximab, the first therapeutically available antibody, is directed against CD20, expressed on B cells. Upon treatment, B cells are directly killed by antibody binding, complement and engagement of immune effector cells (1, 2). For effective elimination of the target, the activation of cells capable of effecting antibody-mediated responses is crucially needed, including both myeloid cells and natural killer (NK) cells (3, 4), which bear Fc γ receptors (Fc γ R) that recognize IgG-bound targets.

The Fc γ R family contains multiple members that modulate antibody-mediated responses. In human monocytes and macrophages, there are three activating receptors: Fc γ RIa, Fc γ RIIa and Fc γ RIIIa (5, 6). Both Fc γ RIa and Fc γ RIIIa are present in the membrane in association with the common gamma chain (Fc ϵ RI γ), which bears an immunoreceptor tyrosine-based activation motif (ITAM) (5, 7). Fc γ RIIa contains an intracellular tail with its own ITAM. Recognition of IgG-bound targets results in the aggregation of these activating receptors and phosphorylation of their ITAMs, initiating multiple signaling cascades, including the phosphatidylinositol 3-kinase (PI3K), mitogen-activated protein kinase (MAPKs) and NF- κ B pathways (8, 9). This leads to the production of cytokines and reactive oxygen species, as well as changes in the membrane to facilitate the phagocytosis and destruction of targets. Phagocytosis itself is highly coordinated, with PI3K, RAC1, CDC42 and ARF6 localized to phagocytic cups where actin polymerization advances the cups around the opsonized targets (10).

This response is modulated by the presence of different regulators, including Fc γ RIIb, the Fc γ R with an immunoreceptor tyrosine-based inhibitory motif (ITIM) instead of an ITAM. Thus, activation of monocytes and macrophages involves a balance between ITAM and ITIM signaling (11). Modulation of this balance, for example by favoring the expression of activating receptors, is of great importance for driving stronger responses to therapeutic antibodies *in vivo* (12, 13). Due to its importance, novel therapeutic antibodies have been widely engineered to enhance the binding to Fc γ R and thus activate cells in a more efficient manner (14, 15).

It is known that innate immune responses are broadly suppressed in cancer. In chronic lymphocytic leukemia (CLL), myeloid cells express higher amounts of regulatory molecules (16) and show decreased expression of some molecules related to antibody-mediated phagocytosis (17). This impedes proper activation upon antigen binding. More importantly, monocytes can differentiate into nurse-like cells (NLCs), which are macrophages widely known to support the survival and drug resistance of CLL cells (18–20). Thus, addressing the suppressive phenotype of myeloid cells is crucial to elicit better antibody-mediated responses in CLL.

To increase their anti-tumoral activity, monocytes/macrophages can be stimulated by various agonists of pattern recognition receptors (PPRs). The Toll-like receptor (TLR) 7 agonist imiquimod has been successfully used to induce myeloid cell activity in melanoma (21). The TLR8 agonist motolimod has been tested against head and neck squamous cell carcinoma in mice and humans (22, 23), and is showing preclinical efficacy against acute myeloid leukemia (AML) (24). Many other PRR agonists are currently being examined (25), while only three of them (BCG, monophosphoryl lipid A, and imiquimod) are currently used against oncologic diseases (26–28).

The potential benefits of treating CLL with PRR agonists have been previously explored. Of note, several reports support an effect of TLR9 agonists towards CLL-cell phenotypic change, increased cytokine production, and apoptosis (29–31). However, CpG 7909 in a phase I clinical trial did not result in a clear response, and testing of CpG 2006 showed that it may halt T cell proliferation (32, 33). Thus, further exploration of PRRs for CLL is needed.

The aforementioned TLRs are intracellular sensors that help detect threats inside the cell (34). Additional PRRs with this function include the nucleotide-binding oligomerization domain-containing 1 and 2 (NOD1 and NOD2) receptors, which recognize peptidoglycans found in both Gram-negative and Gram-positive bacteria (35). Muramyl dipeptide has been found to be the minimal unit that can activate NOD2, enhancing the production of humoral responses (36). Upon activation, NOD2 activates different signaling cascades including the inflammasome, NF- κ B and MAPK pathways, leading to a variety of responses including cytokine production (37–39). In myeloid cells, activation of NOD2 has been linked to the production of TNF α , IL-6 and/or IL-1 β (40), increased

cytolytic activity against tumoral cells (41, 42), enhanced production of reactive oxygen species (43) and differentiation from classical to non-classical monocytes (44). The NOD2 agonist muramyltripeptide phosphatidylethanolamine (MTP-PE, Mifamurtide®) has been used therapeutically to treat osteosarcoma patients in Europe (45), while other agonists have been used for different diseases in other parts of the world (46). This supports the potential of NOD2 agonists as therapeutic adjuvants to enhance responses in myeloid cells. These agonists have also been explored for the treatment of other malignancies including AML (47, 48).

Here, we investigated the role of NOD2 activation in monocyte/macrophage antibody-mediated responses against CLL. We found that the NOD2 agonist L18-MDP activated CLL-patient monocytes, promoting the production of cytokines and an increase in the expression of FcγRs both at the transcript and protein levels. This was highly correlated to an increase in antibody-mediated phagocytosis. These effects were mediated by the NF-κB and MAPK/p38 pathways. Furthermore, we observed that NOD2 agonist treatment led to a decreased leukemic load and a shift in the phenotype of monocytes/macrophages within the Eμ-TCL1 mouse model of CLL. Finally, the agonist significantly enhanced the effects of antitumor antibody. Collectively, these results suggest that NOD2 agonists may carry potential as adjuvants for antibody therapy in CLL.

2 Methodology

2.1 Cell culture

Healthy-donor (HD) source leukocytes were purchased from Versiti Blood Services (Columbus, OH, USA). Whole-blood samples from untreated, low-count (<60,000 cells/μL) CLL patients were provided by the Leukemia Tissue Bank of The Ohio State University Comprehensive Cancer Center, obtained according to the Declaration of Helsinki and under protocols approved by the Institutional Review Board at The Ohio State University. Peripheral blood mononuclear cells (PBMCs) were isolated from each sample using lymphocyte separation medium (Corning, Corning, NY, USA), followed by density gradient centrifugation, and then washed with RPMI (Gibco, Thermo-Fisher Scientific, Waltham, MA, USA). For PBMC experiments, cells were counted using the Cellometer Auto 2000 (Nexcelom Biosciences, Lawrence, MA, USA) and resuspended in RPMI media supplemented with 10% FBS (VWR, Radnor, PA, USA), 2 mM L-glutamine (Gibco) and 100 U/mL Penicillin-Streptomycin (Gibco) at 10x10⁶ cells/mL.

To obtain HD or CLL-patient monocytes (CD14⁺ cells), as well as CLL cells (CD19⁺), PBMCs were incubated with magnetic CD14⁺ or CD19⁺ selection beads (Miltenyi Biotec, Waltham, MA, USA) for 15 minutes on ice. Following this, cells were centrifuged and resuspended in MACS buffer (Miltenyi Biotec) and added to an LS selection column. After three washes, cells were recovered from the column, washed with incomplete RPMI, counted, and resuspended at 3x10⁶ cells/mL in supplemented RPMI media.

For stimulation, cells were plated and treated with L18-MDP (MDP) (InvivoGen, San Diego, CA, USA). A concentration of 1 μg/mL was selected after testing a concentration-response curve in isolated

monocytes, and is similar to a previous report (49). Cells were incubated at 37°C, 5% CO₂, for 24 hours unless indicated otherwise. For inhibition experiments, monocytes were treated with DMSO (as inhibitor vehicle control) or: Bay 11-7085 at 5 μM (Millipore Sigma, St. Louis, MO, USA), trametinib at 10 nM (Selleck Chemicals, Houston, TX, USA), or SB202190 at 1 μM (Selleck Chemicals) for 30 minutes before MDP stimulation. Dimethyl sulfoxide (DMSO; Sigma Aldrich, St. Louis, MO, USA) was used to prepare stock solutions and the final concentration of DMSO was under 1 μL/mL.

2.2 Quantitative real-time PCR

Cultured cells were collected and then mRNA extracted using the Norgen Total RNA extraction kit (Norgen Biotek, ON, Canada), according to the manufacturer's instructions. Collected mRNA was quantified using the nanodrop ND100 (Thermo-Fisher Scientific), and then reverse transcribed using the high-capacity reverse transcriptase kit (Applied Biosystems, Thermo-Fisher Scientific) into cDNA. Then, quantitative real-time PCR (qPCR) was done using SYBR green (Applied Biosystems) and the QuantStudio™ 3 machine (Life Technologies). RCN (relative copy number) values were calculated for each target, normalizing to a GAPDH housekeeping control according to the equation $RCN = 2^{-(\Delta Ct)} \times 100$, where $\Delta Ct = Ct_{problem} - Ct_{GAPDH}$ (50). Primers used are shown in Table 1.

2.3 Immunoblot analysis

Cells were collected and lysed using 70 μL TN1 lysis buffer for every 1 x 10⁶ cells, as previously described (51). Protein was quantified using the DC Protein Assay according to manufacturer's instructions (Bio-Rad, Hercules, CA, USA). Samples were boiled with 5x SDS sample buffer (150 mM Tris; 11.5% SDS; 0.05% bromophenol blue; 50% glycerol; 1% 2-mercaptoethanol). Samples were then size-separated using SDS-PAGE. Proteins were transferred to a nitrocellulose membrane using the Trans-Blot Turbo Transfer System (Bio-Rad). Membranes were blocked with the LI-COR blocking solution (LI-

TABLE 1 Quantitative real-time PCR primers used.

	Forward	Reverse
GAPDH	ACTTTGGTATCGT GGAAGGACT	GTAGAGGCAGGGATG ATGTTCT
FcγRIa	GGCAAGTGGACAC CACAAAGGCA	GCTGGGGTTCGAGG TCTGAGT
FcγRIIa	TTGCTGCTGCTGG CTTCTGC	GTAGCTGGGCTGCG TGTGGG
FcγRIIb	TGACTGCTGTGCT CTGGGCG	AGCCTTTGGGGGA GCAGGTGT
FcγRIIIa	CCTCTCCACCCTCA GTGACCCG	TGAGCAACAGCCA GCCGAT
FcεR1γ	CAAGCAGCGGCC CTGGGAG	TTCCTGGTGCTCA GGCCCGT

COR Biotechnology, NE, USA) and incubated with primary antibodies overnight at 4°C in LI-COR antibody diluent. The following primary antibodies were utilized: phospho-p42/44 (polyclonal, product #9101; or clone D13.14.4E; Cell Signaling Technology), phospho-MAPKAPK2 (polyclonal, product #3041; Cell Signaling Technology), phospho-p38 (clone D3F9; Cell Signaling Technology), phospho-p65 (clone 93H1; Cell Signaling Technology) mouse anti-human GAPDH (clone D4C6R; Cell Signaling Technology), rabbit anti-human FcεRIγ (product 06-727; Upstate, Sigma-Aldrich), and mouse anti-human calreticulin (clone FMC 75, Enzo Life Sciences, Farmingdale, NY, USA). After probing with the corresponding fluorescently-conjugated secondary antibody (IRDye 800CW goat anti-rabbit, or IRDye 680RD goat anti-mouse antibodies; LI-COR) for 1 hour at room temperature, membranes were developed using the Odyssey CLx (LI-COR). For densitometry analysis, Fiji was used (52).

2.4 Flow cytometry

After PBMC or monocyte stimulation, cells were collected and washed with PBS. Then, cells were transferred into v-bottom plates and incubated with whole human IgG (Jackson ImmunoResearch Labs, West Grove, PA, USA) at 10 μg/mL in PBS for 15 minutes on ice. After Fc block, the specific antibody cocktail was added (Table 2). Samples were acquired using the LSR-Fortessa (BD Biosciences) at the Flow Cytometry Shared Resource at The Ohio State University Comprehensive Cancer Center and analyzed using FlowJo version 10.7.2 (Ashland, OR, USA). Supplementary Figure 1 shows an example of the gating used in monocyte analysis.

2.5 ELISA

Cultured cells were centrifuged, and cleared supernatants collected and used for ELISA with the Human TNFα DuoSet ELISA kit (R&D Systems, Minneapolis, MN, USA) according to manufacturer's instructions. For acquisition, the BioTek Synergy HTX plate reader was used (Agilent, Santa Clara, CA, USA).

2.6 Antibody-mediated binding (rosetting)

To determine antibody-mediated binding of targets, opsonized sheep red blood cells (sRBCs; Colorado Serum Company, Denver, CO, USA) were prepared as previously described (53). sRBCs were washed with PBS until the supernatant appeared clear. Then, 2 μL of PKH26 Red Fluorescent Dye (Sigma-Aldrich), diluted in Diluent C, were added to the cell pellet and thoroughly mixed. The reaction was stopped with a 1:1 volume of FBS, and sRBCs were washed with PBS until clear. Fluorescent sRBCs were then opsonized with rabbit anti-sheep antibody (Sigma-Aldrich) on ice for 2 hours before washing.

Upon monocyte stimulation with MDP at 1 μg/mL for 24 hours, cells were used for rosetting analysis, as previously described

TABLE 2 Flow cytometry panels.

Panel	Cocktail
Panel 1: Monocyte activation	CD14 Alexa Fluor 647 (clone HCD14, BioLegend) CD38 FITC (clone HIT2, BioLegend) CD163 PeCy7 (clone GHI/61, BioLegend) CD86 PE (clone BC96, BioLegend) HLA-DR PercP (clone L243, BioLegend) Live/Dead Blue (Thermo-Fisher Scientific)
Panel 2: T cell activation	CD3 Pacific Blue (clone OKT3, BioLegend) CD4 Brilliant Violet 711 (clone RPA-T4, BioLegend) CD8 PercP (clone SK1, BioLegend) CD69 Alexa Fluor 488 (clone FN50, BioLegend) CD25 PeCy7 (clone BC96, BioLegend) CD86 APC (clone IT2.2, BioLegend) Live/Dead Blue
Panel 3: B and NK cell activation	CD19 PeCy7 (clone HIB19, Invitrogen) CD69 Alexa Fluor 488 CD86 APC CD56 Super Bright 600 (clone NCAM, Invitrogen) CD107a PE/Dazzle (clone H4A3, Invitrogen) Live/Dead Blue
Panel 4: FcγRs	CD64 (FcγRIa) PercP Cy5.5 (clone 10.1, BioLegend) CD32a (FcγRIIa) FITC (clone IV.3, StemCell Technologies, Vancouver, Canada) CD32b (FcγRIIb) PeCy7 (clone S18005H, BioLegend) CD16 (FcγRIIIa) Brilliant Violet 711 (clone 3G8, BioLegend) Live/Dead Blue
Panel 5: CLL cells (Mouse model)	CD45 Brilliant Violet 421 (clone 30-F11, BioLegend) CD19 PE (clone 1D3/CD19, BioLegend) CD5 Alexa Fluor 647 (clone 53-7.3, BioLegend) Live/Dead Blue.
Panel 6: Monocyte/macrophage phenotype (Mouse model)	CD45 Brilliant Violet 421 CD11b Brilliant Violet 711 (clone M1/70, BioLegend) Ly6G PerCP (clone 1A8, BioLegend) Ly6C PeCy7 (clone HK1.4, BioLegend) F4/80 Brilliant Violet 605 (clone BM8, BioLegend) IA-IE Brilliant Violet 785 (clone M5/114.15.2, BioLegend) iNOS PE (clone CXNFT, Invitrogen) EGR2 APC (clone Erongr2, Invitrogen) Live/Dead Blue

(53). Briefly, monocytes were divided and incubated with 1 uL of packed, opsonized or non-opsonized, fluorescent sRBCs. Cells were mixed and spun down, then incubated on ice for 1 hour. After incubation, cells were fixed with 1% paraformaldehyde in PBS for 15 minutes before analysis. The number of bound targets per 100 monocytes, as well as the percent of active cells (monocytes with bound sRBCs) were counted through microscopy using the Olympus BX41 (Olympus Life-Science/Evident, Tokyo, Japan). Samples were counted in a blinded fashion by two

different subjects. The number of bound non-opsonized targets in control samples was subtracted from the number of bound opsonized targets.

2.7 Antibody-mediated phagocytosis

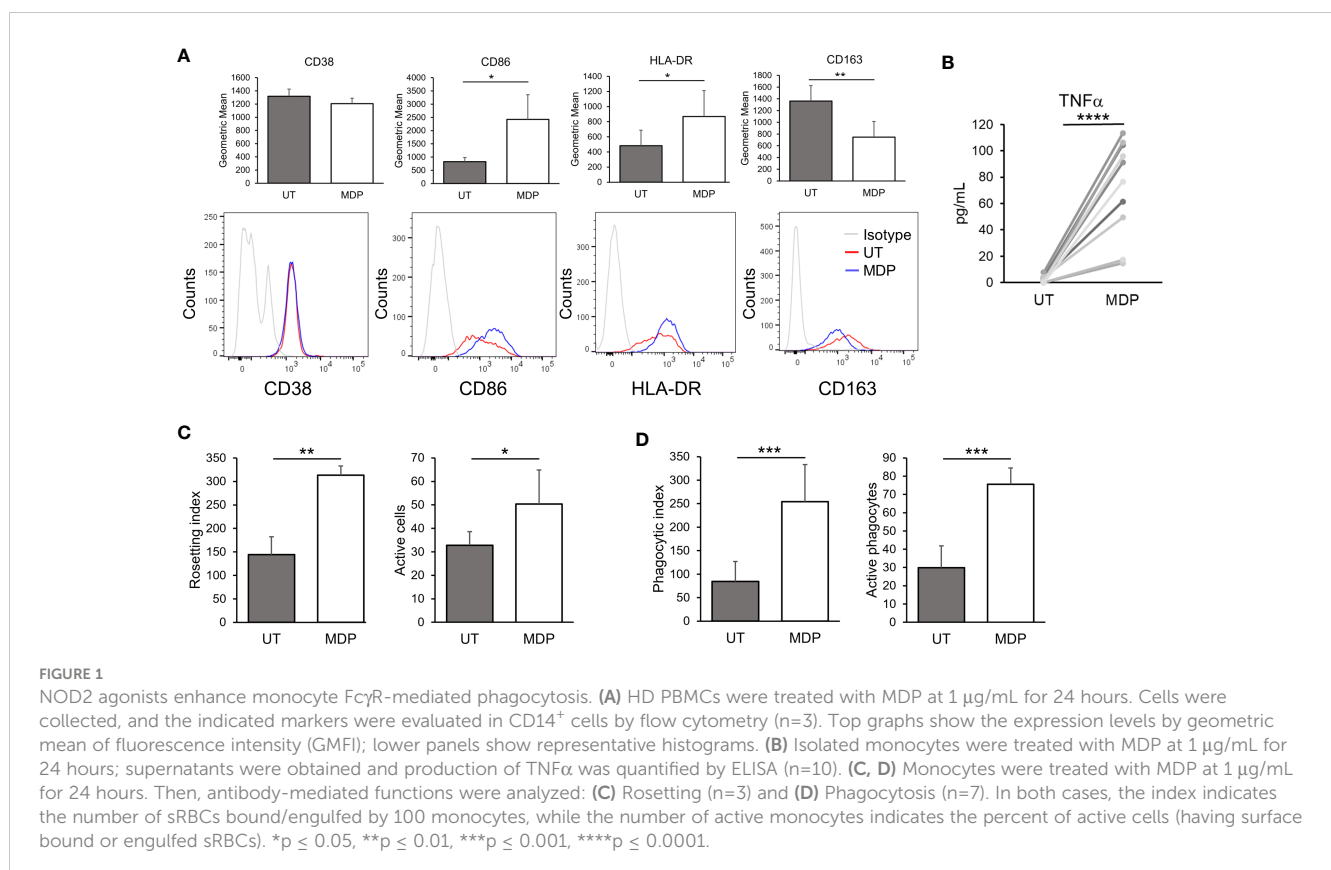
sRBCs were stained with the pH sensitive Protonex Red 600 dye (AAT Bioquest, Pleasanton, CA) at 4 μM in Hanks Buffered Saline Solution (HBSS; Gibco). The staining was done for 30 minutes at 37°C and then sRBCs were washed 3 times with PBS. sRBCs were then opsonized with antibody as stated above.

For measuring phagocytic activity, monocytes were treated with DMSO or pathway inhibitors for 30 minutes before stimulation with MDP at 1 $\mu\text{g}/\text{mL}$ for 24 hours. Then, cells were washed and stained for contrast with carboxyfluorescein succinimidyl ester (CFSE, Thermo-Fisher Scientific) at 0.5 μM in PBS for 10 minutes at room temperature; the reaction was stopped with FBS and cells spun down. Cells were resuspended in complete media to perform the assay. Monocytes were mixed with 1 μL of packed, fluorescently-labeled, opsonized sRBCs for 45 minutes at 37°C, then washed and fixed with paraformaldehyde at a final concentration of 1%. The amount of phagocytosed sRBCs was counted per 100 cells under the microscope, and the number of cells with ingested events was also recorded as active phagocytes. The counts were done

independently by two or three different subjects in a blinded fashion and averages calculated. As control, phagocytosis of non-opsonized, fluorescent sRBCs was checked for negativity. Some donors and results are shared among different phagocytosis assays.

2.8 Mouse model

Mice were housed in a vivarium at The Ohio State University, following all institutional guidelines. All experimental procedures were approved by The Ohio State University Institutional Animal Care and Use Committee. An adoptive transfer E μ -TCL1 mouse model of CLL was used (54, 55). Briefly, 1×10^7 splenocytes from CLL-burdened E μ -TCL1 mice were used to engraft C57BL/6 mice. After 2 weeks of disease development, treatments (5 mg/kg of MDP and/or 1 mg/kg $\alpha\text{CD}20$ (Invivogen, San Diego, CA, USA, catalog #mcd20-mab10 -)) were delivered intraperitoneally three times weekly, for 2 weeks. Engrafted C57BL/6 mice, left untreated, and nongrafted C57BL/6 mice served as controls. Mice were euthanized using a CO $_2$ chamber, followed by cervical dislocation. Spleens and peripheral blood were collected. For spleens, the tissue was weighed and disrupted using a 100 μm cell strainer (Corning); erythrocytes from both blood and disaggregated spleens were eliminated by centrifugation using lymphocyte separation medium. Cells were washed, resuspended in PBS and used for flow cytometry staining.



For flow cytometry staining, cells were placed in a v-bottom plate and stained as above using the antibodies listed for Panels 5 and 6 (Table 2). For monocyte and macrophage phenotyping (Panel 6, iNOS and EGR2), we used the Foxp3 Intracellular staining kit (Thermo-Fisher Scientific) according to the manufacturer's instructions, as described previously (56–58). For acquisition, Absolute Count Beads (BioLegend) were used.

2.9 Statistical analysis

Graphs were prepared using Excel (Microsoft Corporation, Redmond, WA). For two-group comparisons, a one-tailed t-test analysis for paired samples was performed using Excel. For multi-group comparisons, data were analyzed with the mixed effects model using SAS 9.4 (SAS Institute, Cary, NC, USA). Statistical analyses included only the engrafted groups (vehicle, MDP, α CD20 and combination) for mouse experiments, nongrafted controls were not compared. Data in graphs is shown as mean + standard deviation (S.D.).

3 Results

3.1 NOD2 agonists influence the phenotype of monocytes and enhance Fc γ R-mediated phagocytosis

Monocytes and macrophages are well-known responders to NOD2 agonists (40–42). To confirm this, we first treated PBMCs from HDs with MDP at 1 μ g/mL for 24 hours. Flow cytometry was then used to measure different activation markers in monocytes and lymphocytes to determine which populations show an efficient response to NOD2 agonists. As shown in Figure 1A, monocytes showed a significant increase in CD86 and HLA-DR. Concurrently, there was a significant decrease in the M2-associated marker CD163. These results suggest that monocyte activation was skewed toward a proinflammatory phenotype. In T cells, we found that NOD2 agonist treatment increased CD86 in CD4⁺ T cells, which may suggest a slight activation of this population, as has been suggested previously (59) (Supplementary Figure 2A). B and NK cells were also examined, but only a reduction in NK-cell CD107a was observed (Supplementary Figures 2C, D, respectively). Since changes on monocytes were significant, we decided to further test the effects of NOD2 in isolated monocytes. 24 hours following stimulation of NOD2, monocytes produced robust levels of TNF α , measured in the supernatants (Figure 1B). These results confirm earlier reports that monocytes are activated by NOD2 agonists (40, 49).

We next tested whether NOD2 stimulation would increase the phagocytic ability of monocytes, specifically in the context of Fc γ R-mediated responses. For this, we treated monocytes with MDP at 1 μ g/mL for 24 hours and then incubated them with fluoresceinated, antibody-opsonized sRBCs. Here, cells were subjected to rosetting (initial binding stage of phagocytosis) and ingesting assays. Rosetting was done by incubating monocytes with the sRBCs at 4°C while incubation at 37°C was done in parallel to measure

ingestion. As shown in Figure 1C, there was a significant increase in antibody-mediated binding (rosetting) in agonist-treated monocytes compared to controls, which is also reflected in the number of cells with bound sRBCs. Likewise, the number of ingested, opsonized sRBCs was significantly higher in treated monocytes (Figure 1D). There was also a significant increase in the number of actively phagocytosing monocytes. Taken together these results indicate that NOD2 stimulation leads to an increase in Fc γ R-mediated phagocytosis.

3.2 NOD2 stimulation modulates Fc γ R expression

To test whether the increase in phagocytosis could be accounted for by a change in Fc γ R expression, we isolated monocytes from HDs and treated for 24 hours with vehicle or MDP at 1 μ g/mL. Following this, RNA was isolated and transcripts for Fc γ RIa, Fc γ RIIa, Fc γ RIIIa, Fc ϵ RI γ and Fc γ RIIb (the inhibitory Fc γ R) were evaluated by qPCR. Results (Figure 2A) showed that there was a significant increase in the expression of Fc γ RIIa and Fc γ RIIIa. Contrary to our expectation, however, RNA expression of Fc γ RI was significantly lower in MDP-treated monocytes. Transcripts of Fc ϵ RI γ were significantly increased by MDP treatment (Figure 2B, upper panel). Changes in Fc γ RIIb expression were not significant (Supplementary Figure 3A).

We also measured surface expression of Fc γ Rs by flow cytometry. Consistent with an increase in transcripts, there was a significant increase in surface expression of Fc γ RIIa and Fc γ RIIIa in isolated monocytes after 24 hours with NOD2 agonist treatment (Figure 2C). Surprisingly, the surface expression of Fc γ RI was also significantly increased despite the observed reduction in transcript (Figure 2C). In addition to the increase in the geometric mean of expression of the activating Fc γ Rs, we also observed a slight but significant increase in the percent of monocytes positive for Fc γ RI, as well as an increase of the monocyte population expressing Fc γ RIIIa (Supplementary Figure 4). This indicates a phenotypic change into intermediate or non-classical monocytes after NOD2 stimulation (60).

Because surface expression of Fc γ RI depends on Fc ϵ RI γ (7, 61), we also measured protein levels of Fc ϵ RI γ using immunoblot analysis under the same stimulation conditions. Of note, we detected two bands when measuring Fc ϵ RI γ , which has been seen by other authors previously and may correspond to either dimers or phosphorylation of the protein (7, 62); thus, densitometry analysis was done for both. As shown in Figure 2B (middle panel and lower-panel graph), MDP significantly increased protein levels of Fc ϵ RI γ . Hence, despite reducing the transcript of Fc γ RI, MDP treatment led to greater surface expression of all three activating Fc γ Rs on monocytes.

3.3 NF- κ B and p38 are required for NOD2-mediated effects on Fc γ R

Previous studies have demonstrated that NF- κ B, MEK and p38 are activated downstream of NOD2 (37–39). We therefore explored which of these pathways was required for MDP-mediated changes in Fc γ R expression and function. For this, HD monocytes were isolated and each

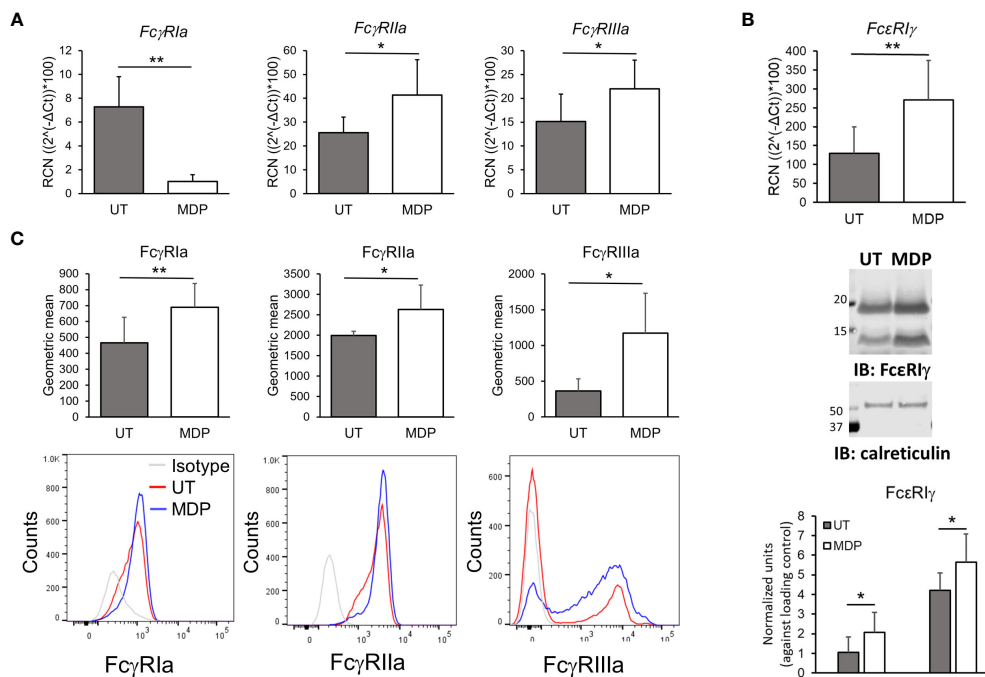


FIGURE 2

NOD2 stimulation modulates FcγR expression. Monocytes were treated for 24 hours with MDP at 1 mg/mL. Cells were collected to analyze (A) transcripts (n=5) and (B) surface expression (n=6) of the FcγRs by qPCR or flow cytometry, respectively. Bottom histograms show a representative donor. (C) mRNA and total protein level of the common gamma chain (FcεR1γ) were evaluated through qPCR and western blot (n=5). *p < 0.05, **p < 0.01.

of these three pathways was inhibited using pharmacologic inhibitors prior to treating the monocytes with MDP. To verify efficacy of the inhibitors, immunoblot analysis was performed with phospho-specific antibodies for NF-κB, ERK and MAPKAPK2 (downstream of p38), measured at 24 hours post-treatment (Supplementary Figure 5). [Of note, no visible activation of p38 was detected at this time point after MDP stimulation, which may be due to p38 activity peaking earlier after stimulation (63–65)]. qPCR and flow cytometry were done to measure FcγR expression. As shown in Figure 3A and quantified in Supplementary Figure 6, MDP-driven increases in FcγR surface expression were prevented by inhibition of NF-κB and p38 but not by inhibition of MEK. Changes in transcript after MDP were also largely prevented by inhibition of NF-κB and p38 (Supplementary Figure 7). Consistent with the effects of these inhibitors on changes in FcγR expression, the MDP-mediated increase in phagocytosis was prevented with NF-κB and p38 inhibition (Figure 3B). Taken together, these data demonstrate that NF-κB and p38 are required mediators for enhancing FcγR expression and function downstream of NOD2.

3.4 NOD2 regulates FcγR function in CLL-patient monocytes

CLL-patient monocytes are known to have altered phenotype compared to HDs (17). Thus, to test whether the effects of NOD2 stimulation seen in HD monocytes were reproducible in CLL-patient monocytes, we isolated monocytes from deidentified peripheral blood samples obtained from CLL patients and measured NOD2 expression

using qPCR. As shown in Figures 4A, B, NOD2 was expressed in CLL-patient monocytes at similar transcript levels to HD monocytes. As with HD monocytes, CLL-patient monocytes were able to respond to MDP by producing TNFα after 24 hours of stimulation. Further, MDP treatment of CLL-patient monocytes also enhanced surface expression of FcγRI and FcγRIIIa, observed by flow cytometry (Figure 4C), and expression of FcεR1γ, measured by immunoblot (Figure 4D). In addition, the transcriptional levels of FcγRIIb in CLL-patient monocytes remained unchanged after NOD2 stimulation (Supplementary Figure 3B). However, in contrast to HD monocytes, MDP treatment did not increase surface expression of FcγRIIa in CLL-patient monocytes after MDP treatment (Figure 4C, middle graph). However, consistent with an overall increase in activating FcγRs, MDP treatment of CLL-patient monocytes led to a significantly higher level of phagocytosis (Figure 4E). In contrast to HD monocytes, the same increase in rosetting was not seen in patient monocytes (Figure 4F), although monocytes from 3 of the 4 donors showed higher levels with MDP treatment. This suggests that despite a lower overall response than that seen in HD monocytes, CLL-patient monocytes are capable of responding to MDP by increasing FcγR expression, cytokine production and phagocytic ability.

In addition to monocytes, the effect of MDP on CLL cell activation and proliferation in patient samples was examined, as this could be a potential and undesirable side effect. PBMCs from CLL patients were treated with MDP for 24 hours, then expression of CD86 in CLL cells was measured using flow cytometry. Although there was some increase in CD86, it was not significant (Supplementary Figure 8A). We next isolated B/CLL cells and treated with vehicle or MDP, counting cell numbers and viability

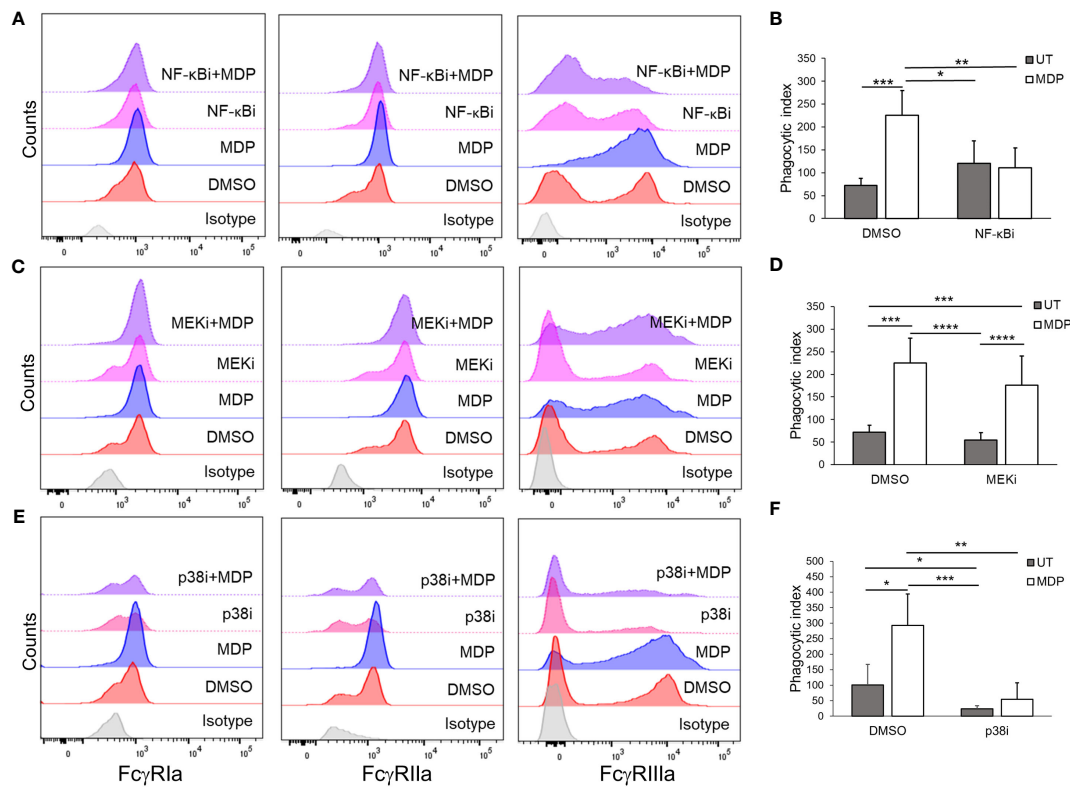


FIGURE 3

NF-κB and p38 are required for NOD2-mediated effects on FcγR. Monocytes were treated with inhibitors against (A, B) NF-κB, (C, D) MEK, (E, F) or p38 for 30 minutes, before stimulation with MDP for 24 hours. Following incubation, (A, C, E) expression of the FcγRs was measured through flow cytometry (representative histogram of $n \geq 4$ is shown); (B, D, F) antibody-mediated phagocytosis was evaluated ($n \geq 3$). * $p \leq 0.05$, ** $p \leq 0.01$, *** $p \leq 0.001$, **** $p \leq 0.0001$.

at different time points. As shown in **Supplementary Figures 8B, C**, the viability of CLL cells was not affected by MDP. These results suggest that NOD2 activation does not affect CLL cell viability. Taking cell number and percent viability together, results also suggest that MDP did not directly affect CLL-cell proliferation.

3.5 NOD2 activation enhances effects of antitumor antibody *in vivo*

To test the effects of NOD2 stimulation on FcγR function *in vivo*, we used a mouse model that mimics human CLL (66, 67). C57/BL6 mice were engrafted with splenocytes from diseased Eμ-TCL1 mice, as described in the methodology. Disease was allowed to develop for 2 weeks. Animals were either treated with vehicle, treated with MDP, treated with a suboptimal dose of αCD20 antibody or treated with MDP plus αCD20 antibody in combination. Mice were sacrificed after 2 weeks of treatment. Healthy, nonengrafted mice were included as controls. CLL loads in peripheral blood and in the spleens were assessed. Results showed that white blood cell (WBC) counts in peripheral blood were significantly reduced by each single treatment, and dual treatment led to greater reduction than either single treatment (**Figure 5A**). There was also a significantly lower percentage of CD5⁺/CD19⁺ CLL cells after antibody treatment, and dual treatment led to a lower percentage than either single treatment (**Figure 5B**).

In addition to the leukemic load in the blood, we analyzed the spleen, as CLL cells tend to accumulate in this organ (68). Spleen weights were also significantly lower in mice treated with antibody, but MDP plus antibody led to spleen weights significantly lower than those for untreated or for either single treatment (**Figure 5C**). The number of CLL cells per milligram of spleen weight (**Figure 5D**) was also significantly lower with dual treatment compared to either single treatment or vehicle control. Furthermore, this was also observed in the percent of CD19⁺CD5⁺ cells from the viable CD45⁺ population (data not shown). An image of the spleens is shown in **Figure 5E**. These results suggest that the combination of NOD2 agonist plus therapeutic antibody may be more effective than antibody alone.

3.6 NOD2 agonists shift monocyte/macrophage phenotype *in vivo*

In addition to the leukemic burden, we tested whether MDP combined with antitumor antibody could modulate the phenotypes of monocytes and macrophages *in vivo*. For this, cells from the spleen were obtained and stained for flow cytometry to detect M1- and M2-related markers on monocytes and macrophages. Cells were gated as CD45⁺CD11b⁺Ly6G⁻ and further classified by expression of MHC-II and/or F4/80 as previously done (56). Percentages of cells expressing iNOS (M1) or EGR2 (M2) (58)

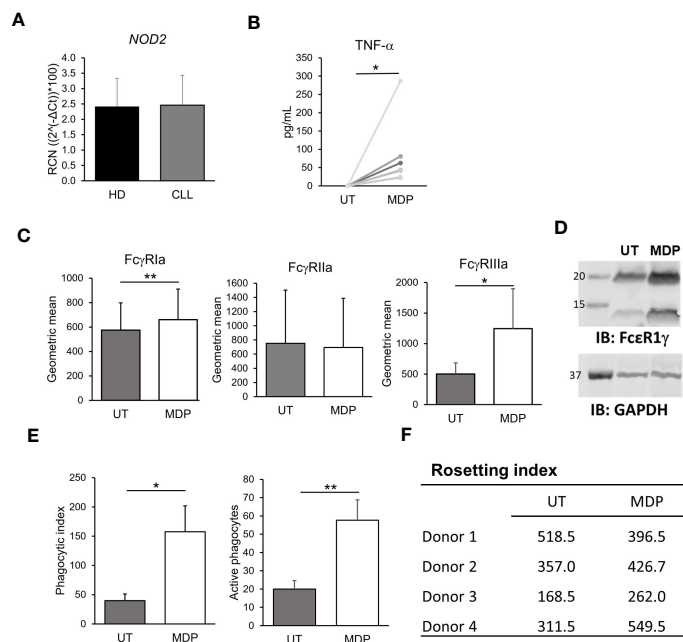


FIGURE 4 NOD2 regulates FcγR expression function in CLL-patient monocytes. (A) Levels of NOD2 expression in HD and CLL-patient monocytes were measured by qPCR (n=5 donors each). CLL-patient monocytes were stimulated for 24 hours with MDP at 1 μg/mL and (B) production of TNFα was evaluated in the supernatant (n=8); (C) levels of FcγRs were measured by flow cytometry (n=6) or (D) FcεR1γ abundance was observed by western blot (representative blot, n=3 donors). (E) Antibody-mediated phagocytosis (n=3), or (F) Rosetting (n=4) were also measured. *p ≤ 0.05, **p ≤ 0.01.

were measured to assess M1 or M2 polarization. Results from nonengrafted, healthy control mice were also collected.

In MHC-II⁺ populations either negative or positive for F4/80 (mainly monocytes or macrophages, Figures 6A, B, respectively) there was a significant upregulation of iNOS with either single treatment, and dual-treatment led to significantly higher M1 marker iNOS than either single treatment or vehicle. Neither single treatment significantly downregulated the percent of myeloid cells expressing the M2 marker EGR2, but dual-treatment significantly reduced EGR2 compared to vehicle control and compared to either single treatment. In the F4/80⁺ group (Figure 6C), all treatments led to significantly higher iNOS versus vehicle, and combination treatment led to significantly higher iNOS than antibody-alone treatment. Taken together, these data suggest that MDP/antibody combination treatment not only decreases CLL burden but also shifts myeloid phenotypes towards a more proinflammatory, and potentially M1-like state.

4 Discussion

In the present study, we report for the first time the potential for NOD2 agonists to offset the suppressive leukemic microenvironment and enhance antibody-mediated responses in CLL. MDP led to enhanced responses *in vitro* in monocytes from CLL patients, although these responses do not entirely mimic the observations

seen in HD cells. This may be related to the overall altered phenotype of myeloid cells seen in CLL, and the role they have as leukemia-supportive cells (16–20, 56). Of note, MDP significantly enhanced the activity of αCD20 antibody *in vivo*, leading to lower tumor burden and a shift towards a proinflammatory phenotype in monocytes and macrophages.

The activation of monocytes in both HD and CLL-patient samples after NOD2 stimulation led to a significant increase in the expression of activating FcγRs. Previously, it has been shown that NOD2 promotes a phenotypic change from classical to non-classical monocytes, which involves an increase of FcγRIIIa (44). This observation is in line with ours and, in addition, we also saw a significant increase in the surface expression of FcγRIa, likely being stabilized by the common gamma chain (61). In combination with our observations of increased expression of HLA-DR and CD86, along with lower expression of CD163, these results suggest a shift towards an intermediate phenotype of monocytes after NOD2 stimulation (60). The increase in expression of activating FcγRs in the membrane is of importance, since patients with active CLL have a dominance of FcγRIIb signaling, which can lead to decreased antibody-mediated activity (5, 69, 70). In addition, FcγRs are crucial for αCD20 antibody efficacy *in vivo* (69, 71). Thus, using a NOD2 agonist in combination with a therapeutic antibody may overcome resistance to the antibodies. This is supported further by the increase in phagocytosis seen in both HD and CLL-patient monocytes, which is one of the main mechanisms for elimination

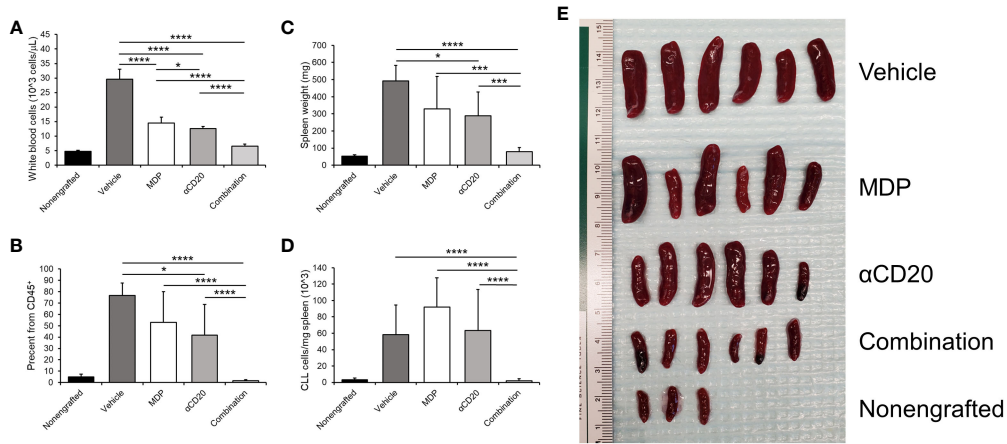


FIGURE 5

NOD2 activation enhances effects of antitumor antibody *in vivo*. Mice were engrafted with splenocytes from a diseased Eμ-TCL1 mouse and disease was allowed to develop for two weeks. Mice were treated with MDP, αCD20 antibody or a combination three times per week for two weeks. Mice were then euthanized, and blood and spleen samples obtained. (A) White blood cell counts were taken as explained in the methods. (B) Percent CD19⁺CD5⁺ cells in CD45⁺ peripheral blood was measured by flow cytometry and graphed. (C) Spleen weights were taken, and (D) number of CD45⁺CD19⁺CD5⁺ cells per milligram spleen weight was measured (n=3 for nonengrafted, n=6 for all others). (E) Picture depicting the spleens from the indicated groups is shown. *p < 0.05, ***p < 0.001, ****p < 0.0001.

of αCD20-opsonized targets by myeloid cells, and has been observed *in vivo* in B cell lymphoma (72). Further experiments are ongoing to elucidate the effects of NOD2 stimulation in NLCs from CLL patients.

We also observed that NOD2 stimulation may not only influence antibody-mediated responses, but also myeloid cells within the microenvironment. Using the adoptive transfer

Eμ-TCL1 mouse model, we saw a significant decrease of the disease burden in mice treated with the combination, in comparison with either single treatment, both in circulation and in the spleen. Most importantly, we also observed an increase of the percent of monocytes or macrophages that expressed iNOS. This effect was even greater when mice were treated with both MDP and αCD20 antibody, compared with either treatment alone. In addition, the

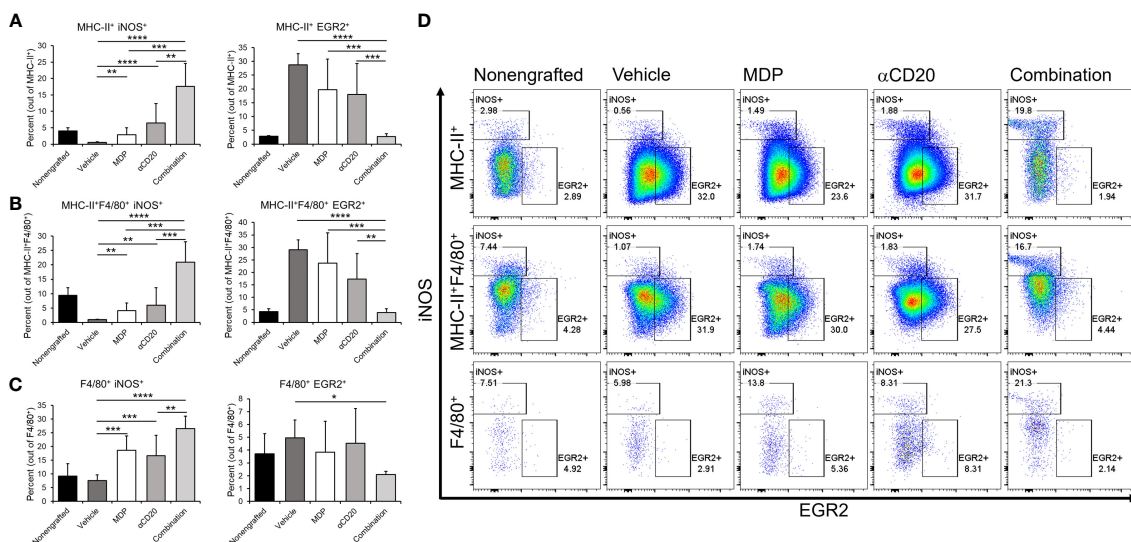


FIGURE 6

NOD2 agonists shift monocyte/macrophage phenotype *in vivo*. C57BL/6 mice were engrafted with splenocytes from a diseased Eμ-TCL1 mouse and the disease was allowed to develop for two weeks. Mice were treated with MDP, αCD20 antibody or a combination three times a week for two weeks. Then, mice were sacrificed, and spleen samples obtained. Cells were stained for flow cytometry and monocytes/macrophages were identified as CD45⁺CD11b⁺+Ly6G⁻ cells and divided by F4/80 and/or MHC-II expression. (A) MHC-II⁺, (B) MHC-II⁺F4/80⁺ and (C) F4/80⁺ cells were then characterized as M1 by iNOS expression, or as M2 by EGR2 expression. Percents of M1 or M2 in the different populations are shown. (D) Representative dot plots from one mouse per group for iNOS/EGR2 expression are shown (n=3 for unengrafted, n=6 for all others). **p < 0.01, ***p < 0.001, ****p < 0.0001.

combination treatment was the only one that reduced the percent of EGR2⁺ monocytes and macrophages, suggesting that dual treatment was needed to overcome the suppressive environment. Of note, NOS2 or iNOS have been widely attributed to M1-related IFN γ stimulation, while higher EGR2 expression is highly correlated with M2-like responses (57, 58). Thus, the iNOS response to dual treatment suggests an active switch in the phenotype of myeloid cells.

There are different mechanisms that may play a role in the change in monocytes/macrophages' phenotypic differences, as well as the reduced leukemic burden, which are observed in the combination treatment. First, the combination may result in an increase in Fc γ Rs as seen in human patient samples, or perhaps other factors involved in downstream signaling cascades are shared between the two processes. For example, the downstream mediator RIP2 has been shown to be common between NOD2 and Fc γ R, although knockout of RIP2 did not lead to defects in IgG2a-driven Fc γ R signaling (73), and the mouse α CD20 antibody used in the current study was based on IgG2a. In addition, signals like NF- κ B or MAPK happen through activation of Fc γ Rs or NOD2, while an increase in IFN γ production has been suggested for NOD2 mediated stimulation (74). Further research is currently in progress to delineate the mechanism of action of the combination.

It has been previously suggested that NOD2 activation may result in a variety of outcomes in myeloid cells, depending on the agonists used (42). Mifamurtide® has been shown to induce monocyte activation in treated patients, (reviewed in (45)), which involved production of cytokines and direct cytotoxicity against tumoral cell lines (75–77). In addition, macrophages polarized *in vitro* with GM-CSF and further activated with MTP-PE and IFN γ are capable of inhibiting osteosarcoma growth by producing soluble factors, although independent of TNF α or IL-1 β (78). Dieter et al. showed that MTP-PE could induce TNF α and nitric oxide from liver macrophages and that MTP-PE-stimulated macrophages showed direct cytotoxic effects against the P815 mouse mastocytoma cell line (79). Our observation of TNF α production following MDP treatment further supports these observations, while translating our observations to other diseases and potentially other diseases may be carefully considered.

There is concern that MDP may have effects apart from promoting myeloid-cell activation. A previous report showed that MDP increased activation and survival of CLL cells in a specific group of patients, which may be an undesired side effect (80). However, we did not see a substantial activation of B cells in HD or CLL patients (as measured by CD86 expression), either as isolated cells or in PBMC cultures. In line with these observations, MDP alone does not increase the leukemic load *in vivo*. Although results may differ due to the use of different stimulation approaches, our observation suggests that the use of NOD2 agonists for CLL treatment does not result in leukemic progression.

Along with this, the benefits of NOD2 agonists seem to outweigh such potential unwanted effects when used against other types of cancer. Mifamurtide® has been used for the treatment of

osteosarcoma in Europe. In 2009, the European Medicines Agency granted Takeda marketing approval, based on the INT-0133 clinical trial (45). The trial examined the effects of MTP-PE with chemotherapeutic agents, finding that MTP-PE plus a four-drug chemotherapy regimen (doxorubicin, ifosfamide, cisplatin and methotrexate) showed the best event-free survival (81). Further studies have been done to complement observations from the INT-0133 trial (82). The use of this NOD2 agonist is approved for youth populations (2 to 30 years of age) as follow-up treatment after surgical removal of the main affected tissue (45).

In conclusion, the present study provides evidence that combination therapy of α CD20 antibody and NOD2 agonists may be useful to overcome antibody resistance and to promote the elimination of leukemic cells in CLL. This may also be of benefit for patients who acquired resistance to BTK inhibitors or to other therapies. Further research is required to elucidate the specific mechanisms by which NOD2 agonists reverse suppression in myeloid cells, especially in combination with Fc γ R activation.

Data availability statement

The raw data supporting the conclusions of this article will be provided openly by the authors upon request.

Ethics statement

The studies involving humans were approved by The Ohio State University Institutional Review Board under OSU-1997C194. The studies were conducted in accordance with the local legislation and institutional requirements. The participants provided their written informed consent to participate in this study. The animal study was approved by The Ohio State University Institutional Animal Care and Use Committee. The study was conducted in accordance with the local legislation and institutional requirements.

Author contributions

GM-R: Formal analysis, Investigation, Project administration, Visualization, Writing – original draft, Writing – review & editing. MFB: Investigation, Visualization, Writing – original draft, Writing – review & editing. RS: Investigation, Visualization, Writing – review & editing. MV-P: Investigation, Visualization, Writing – review & editing. RM: Investigation, Visualization, Writing – review & editing. AC: Investigation, Visualization, Writing – review & editing. X-MM: Formal Analysis, Visualization, Writing – review & editing. FR-A: Investigation, Resources, Writing – review & editing. JR-R: Investigation, Resources, Visualization, Writing – review & editing. WC: Conceptualization, Resources, Writing – review & editing. JCB: Conceptualization, Resources, Writing – review & editing. JW: Methodology, Resources, Writing – review & editing.

ST: Conceptualization, Funding acquisition, Supervision, Writing – original draft, Writing – review & editing. JPB: Conceptualization, Funding acquisition, Supervision, Writing – original draft, Writing – review & editing.

Funding

The author(s) declare financial support was received for the research, authorship, and/or publication of this article. This work was supported by R01 CA203584 (ST, JPB), K01 DK128379 (JR-R), P30 CA016058 (OSUCCC shared resources) and startup funding from The Ohio State University Comprehensive Cancer Center (JPB). This work was supported by the Pelotonia Scholars Program (MFB). Any opinions, findings, and conclusions expressed in this material are those of the author(s) and do not necessarily reflect those of the Pelotonia Scholars Program or The Ohio State University.

Acknowledgments

We are grateful to Huiqing Fang for critical support during this project.

Conflict of interest

The authors declare that the research was conducted in the absence of any commercial or financial relationships that could be construed as a potential conflict of interest.

The author(s) declared that they were an editorial board member of *Frontiers*, at the time of submission. This had no impact on the peer review process and the final decision.

Publisher's note

All claims expressed in this article are solely those of the authors and do not necessarily represent those of their affiliated organizations, or those of the publisher, the editors and the reviewers. Any product that may be evaluated in this article, or claim that may be made by its manufacturer, is not guaranteed or endorsed by the publisher.

Supplementary material

The Supplementary Material for this article can be found online at: <https://www.frontiersin.org/articles/10.3389/fimmu.2024.1409333/full#supplementary-material>

SUPPLEMENTARY FIGURE 1

General gating strategy for HD or CLL-patient monocytes. For evaluating the expression of the FcγRs in monocytes by flow cytometry, viable cells were selected by (A) first cleaning up doublets (singlet selection). (B) Then, gating was done to exclude debris in the SSC vs FSC dot plot. (C) All cells were stained for viability, so nonviable cells were excluded following SSC vs FSC gating. For monocytes, the geometric mean fluorescence or selection of FcγR-positive populations were done with this sub-gate, subtracting the isotype control signal. A similar strategy was used for evaluation of activation-related proteins in PBMCs, where selection of monocytes, T, B and NK cells was done after (C), staining for population-specific proteins. Depicted is an example healthy-donor monocyte sample.

SUPPLEMENTARY FIGURE 2

Effects of NOD2 stimulation in other immune-cell populations. Isolated PBMCs were treated with MDP at 1 μg/mL for 24 hours. Then, samples were collected, and the indicated markers were analyzed by flow cytometry in viable (A) CD3⁺CD4⁺, (B) CD3⁺CD8⁺, (C) CD19⁺, and (D) CD56⁺ cells (n=3). *p < 0.05, **p ≤ 0.01.

SUPPLEMENTARY FIGURE 3

MDP treatment does not significantly affect FcγRIIb expression. Monocytes from HD (A; n=5) or CLL patients (B; n=7) were treated with MDP at 1 μg/mL for 24 hours. Then, levels of FcγRIIb expression were measured by qPCR. Results are shown as relative copy numbers (RCN).

SUPPLEMENTARY FIGURE 4

NOD2 agonists increase the expression of activating FcγRs. HD monocytes were treated with MDP at 1 μg/mL for 24 hours. Then, cells were collected and evaluated for surface expression of FcγRs. Percentages of positive cells for (A) FcγRIa, (B) FcγRIIa, and (C) FcγRIIIa are shown (n= 6). Top graphs show averages +S.D., while histograms in the bottom panels show a representative donor. *p ≤ 0.05, **p ≤ 0.01.

SUPPLEMENTARY FIGURE 5

Verification of inhibitor activity. Monocytes were treated with inhibitors against (A) NF-κB, (B) MEK or (C) p38. To ensure appropriate blocking, the activation of downstream targets was assessed by western blot. Of note, cells were collected to measure levels of protein phosphorylation 24 hours after stimulation with MDP. Figure shows a representative blot for each inhibitor (n ≤ 3). GAPDH was used as loading control.

SUPPLEMENTARY FIGURE 6

Inhibition of NF-κB and p38 affects monocyte FcγR transcriptional responses to NOD2. Healthy-donor monocytes were treated with inhibitors for (A) NF-κB, (B) MEK and (C) p38 before stimulation with NOD2 agonist for 24 hours. Cells collected, and total RNA obtained. The expression of FcγR was evaluated through qPCR. *p ≤ 0.05, **p ≤ 0.01, ***p ≤ 0.001, ****p ≤ 0.0001 (n ≤ 3).

SUPPLEMENTARY FIGURE 7

Inhibition of NF-κB and p38 affects NOD2-mediated changes in FcγR surface expression in monocytes. HD monocytes were treated with inhibitors for (A) NF-κB, (B) MEK and (C) p38 before stimulation with NOD2 agonist for 24 hours. Cells were collected and the expression of FcγR was evaluated through flow cytometry. Expression was calculated by the geometric mean; the percent of FcγRIIIa positive population is also shown. *p ≤ 0.05, **p ≤ 0.01, ***p ≤ 0.001, ****p ≤ 0.0001 (n ≥ 3).

SUPPLEMENTARY FIGURE 8

MDP stimulation does not induce CLL cell activation and survival *in vitro*. (A) PBMCs from CLL patients were isolated and stimulated with 1 μg/mL MDP for 24 hours. Then, cells were collected and the expression of CD86 in B cells was evaluated by flow cytometry (n=3). Isolated B cells from CLL patients were treated once with MDP at 1 μg/mL; then, the number of (B) viable cells and the (C) percent viability was evaluated at the indicated time points (n=3).

References

- Maloney DG, Grillo-Lopez AJ, White CA, Bodkin D, Schilder RJ, Neidhart JA, et al. IDEC-C2B8 (Rituximab) anti-CD20 monoclonal antibody therapy in patients with relapsed low-grade non-Hodgkin's lymphoma. *Blood*. (1997) 90:2188–95. doi: 10.1182/blood.V90.6.2188.2188_2188_2195
- Reff ME, Carner K, Chambers KS, Chinn PC, Leonard JE, Raab R, et al. Depletion of B cells *in vivo* by a chimeric mouse human monoclonal antibody to CD20. *Blood*. (1994) 83:435–45. doi: 10.1182/blood.V83.2.435.bloodjournal832435
- Rafiq S, Butchar JP, Cheney C, Mo X, Trotta R, Caligiuri M, et al. Comparative assessment of clinically utilized CD20-directed antibodies in chronic lymphocytic leukemia cells reveals divergent NK cell, monocyte, and macrophage properties. *J Immunol*. (2013) 190:2702–11. doi: 10.4049/jimmunol.1202588
- Weiskopf K, Weissman IL. Macrophages are critical effectors of antibody therapies for cancer. *MABS*. (2015) 7:303–10. doi: 10.1080/19420862.2015.1011450
- Bournazos S, Wang TT, Ravetch JV. The role and function of fcγ receptors on myeloid cells. *Microbiol Spectr*. (2016) 4:1–19. doi: 10.1128/microbiolspec.MCHD-0045-2016
- Bruhns P, Jonsson F. Mouse and human FcR effector functions. *Immunol Rev*. (2015) 268:25–51. doi: 10.1111/immr.12350
- Ernst LK, Duchemin AM, Anderson CL. Association of the high-affinity receptor for IgG (Fc gamma RI) with the gamma subunit of the IgE receptor. *Proc Natl Acad Sci U S A*. (1993) 90:6023–7. doi: 10.1073/pnas.90.13.6023
- Patel KR, Roberts JT, Barb AW. Multiple Variables at the Leukocyte Cell Surface Impact Fc gamma Receptor-Dependent Mechanisms. *Front Immunol*. (2019) 10:223. doi: 10.3389/fimmu.2019.00223
- Ben Mkaddem S, Benhamou M, Monteiro RC. Understanding fc receptor involvement in inflammatory diseases: from mechanisms to new therapeutic tools. *Front Immunol*. (2019) 10:811. doi: 10.3389/fimmu.2019.00811
- Swanson JA. Shaping cups into phagosomes and macropinosomes. *Nat Rev Mol Cell Biol*. (2008) 9:639–49. doi: 10.1038/nrm2447
- Getahun A, Cambier JC. Of ITIMs, ITAMs, and ITAMis: revisiting immunoglobulin Fc receptor signaling. *Immunol Rev*. (2015) 268:66–73. doi: 10.1111/immr.12336
- Clynes RA, Towers TL, Presta LG, Ravetch JV. Inhibitory Fc receptors modulate *in vivo* cytotoxicity against tumor targets. *Nat Med*. (2000) 6:443–6. doi: 10.1038/74704
- Wernersson S, Karlsson MCL, Dahlström J, Mattsson R, Verbeek JS, Heyman B. IgG-mediated enhancement of antibody responses is low in fc receptor γ Chain-deficient mice and increased in FcγRII-deficient mice. *J Immunol*. (1999) 163:618–22. doi: 10.4049/jimmunol.163.2.618
- Natsume A, Niwa R, Satoh M. Improving effector functions of antibodies for cancer treatment: Enhancing ADCC and CDC. *Drug Design Dev Ther*. (2009) 3:7–16. doi: 10.2147/DDDT
- DiLillo DJ, Ravetch JV. Fc-receptor interactions regulate both cytotoxic and immunomodulatory therapeutic antibody effector functions. *Cancer Immunol Res*. (2015) 3:704–13. doi: 10.1158/2326-6066.CCR-15-0120
- Hanna BS, Ozturk S, Seiffert M. Beyond bystanders: Myeloid cells in chronic lymphocytic leukemia. *Mol Immunol*. (2019) 110:77–87. doi: 10.1016/j.molimm.2017.11.014
- Maffei R, Bulgarelli J, Fiorcari S, Bertoncelli L, Martinelli S, Guarnotta C, et al. The monocytic population in chronic lymphocytic leukemia shows altered composition and deregulation of genes involved in phagocytosis and inflammation. *Haematologica*. (2013) 98:1115–23. doi: 10.3324/haematol.2012.073080
- Burger JA, Tsukada N, Burger M, Zvaifler NJ, Dell'Aquila M, Kipps TJ. Blood-derived nurse-like cells protect chronic lymphocytic leukemia B cells from spontaneous apoptosis through stromal cell-derived factor-1. *Blood*. (2000) 96:2655–63. doi: 10.1182/blood.V96.8.2655.h8002655_2655_2663
- Boissard F, Fournie JJ, Quillet-Mary A, Ysebaert L, Poupot M. Nurse-like cells mediate ibrutinib resistance in chronic lymphocytic leukemia patients. *Blood Cancer J*. (2015) 5:e355. doi: 10.1038/bcj.2015.74
- Tsukada N, Burger JA, Zvaifler NJ, Kipps TJ. Distinctive features of “nurselike” cells that differentiate in the context of chronic lymphocytic leukemia. *Blood*. (2002) 99:1030–7. doi: 10.1182/blood.V99.3.1030
- Urosevic M, Maier T, Benninghoff B, Slade H, Burg G, Dummer R. Mechanisms underlying imiquimod-induced regression of basal cell carcinoma *in vivo*. *Arch Dermatol*. (2003) 139:1325–32. doi: 10.1001/archderm.139.10.1325
- Cheng Y, Borchering N, Ogunsakin A, Lemke-Miltner CD, Gibson-Corley KN, Rajan A, et al. The anti-tumor effects of cetuximab in combination with VTX-2337 are T cell dependent. *Sci Rep*. (2021) 11:1535. doi: 10.1038/s41598-020-80957-z
- Ferris RL, Saba NF, Gitlitz BJ, Haddad R, Sukari A, Neupane P, et al. Effect of adding motolimod to standard combination chemotherapy and cetuximab treatment of patients with squamous cell carcinoma of the head and neck: the active8 randomized clinical trial. *JAMA Oncol*. (2018) 4:1583–8. doi: 10.1001/jamaoncol.2018.1888
- Yang W, Sun X, Liu S, Xu Y, Li Y, Huang X, et al. TLR8 agonist Motolimod-induced inflammatory death for treatment of acute myeloid leukemia. *BioMed Pharmacother*. (2023) 163:114759. doi: 10.1016/j.biopha.2023.114759
- Shekarian T, Valsesia-Wittmann S, Brody J, Michallet MC, Depil S, Caux C, et al. Pattern recognition receptors: immune targets to enhance cancer immunotherapy. *Ann Oncol*. (2017) 28:1756–66. doi: 10.1093/annonc/mdx179
- Sfakianos JP, Salome B, Daza J, Farkas A, Bhardwaj N, Horowitz A. Bacillus Calmette-Guerin (BCG): Its fight against pathogens and cancer. *Urol Oncol*. (2021) 39:121–9. doi: 10.1016/j.urolonc.2020.09.031
- Wang YQ, Bazin-Lee H, Evans JT, Casella CR, Mitchell TC. MPL adjuvant contains competitive antagonists of human TLR4. *Front Immunol*. (2020) 11:577823. doi: 10.3389/fimmu.2020.577823
- Bubna AK. Imiquimod - Its role in the treatment of cutaneous Malignancies. *Indian J Pharmacol*. (2015) 47:354–9. doi: 10.4103/0253-7613.161249
- Liang X, Moseman EA, Farrar MA, Bachanova V, Weisdorf DJ, Blazar BR, et al. Toll-like receptor 9 signaling by CpG-B oligodeoxynucleotides induces an apoptotic pathway in human chronic lymphocytic leukemia B cells. *Blood*. (2010) 115:5041–52. doi: 10.1182/blood-2009-03-213363
- Wolska A, Cebula-Obrzut B, Smolewski P, Robak T. Effects of Toll-like receptor 7 and Toll-like receptor 9 signaling stimulators and inhibitors on chronic lymphocytic leukemia cells *ex vivo* and their interactions with cladrifine. *Leukemia lymphoma*. (2013) 54:1268–78. doi: 10.3109/10428194.2012.741233
- Decker T, Schneller F, Sparwasser T, Tretter T, Lipford GB, Wagner H, et al. Immunostimulatory CpG-oligonucleotides cause proliferation, cytokine production, and an immunogenic phenotype in chronic lymphocytic leukemia B cells. *Blood*. (2000) 95:999–1006. doi: 10.1182/blood.V95.3.999.003k10_999_1006
- Zent CS, Smith BJ, Ballas ZK, Wooldridge JE, Link BK, Call TG, et al. Phase I clinical trial of CpG oligonucleotide 7909 (PF-03512676) in patients with previously treated chronic lymphocytic leukemia. *Leuk Lymphoma*. (2012) 53:211–7. doi: 10.3109/10428194.2011.608451
- Ringelstein-Harlev S, Avivi I, Fanadka M, Horowitz NA, Katz T. Chronic lymphocytic leukemia cells acquire regulatory B-cell properties in response to TLR9 and CD40 activation. *Cancer Immunol Immunother*. (2018) 67:739–48. doi: 10.1007/s00262-018-2128-x
- Kawasaki T, Kawai T. Toll-like receptor signaling pathways. *Front Immunol*. (2014) 5:461. doi: 10.3389/fimmu.2014.00461
- Ogawa C, Liu YJ, Kobayashi KS. Muramyl dipeptide and its derivatives: peptide adjuvant in immunological disorders and cancer therapy. *Curr Bioact Compd*. (2011) 7:180–97. doi: 10.2174/157340711796817913
- Elloz F, Adam A, Ciorbaru R, Lederer E. Minimal structural requirements for adjuvant activity of bacterial peptidoglycan derivatives. *Biochem Biophys Res Commun*. (1974) 59:1317–25. doi: 10.1016/0006-291X(74)90458-6
- Kobayashi K, Inohara N, Hernandez LD, Galan JE, Nunez G, Janeway CA, et al. RICK/Rip2/CARDIAK mediates signalling for receptors of the innate and adaptive immune systems. *Nature*. (2002) 416:194–9. doi: 10.1038/416194a
- Girardin SE, Travassos LH, Herve M, Blanot D, Boneca IG, Philpott DJ, et al. Peptidoglycan molecular requirements allowing detection by Nod1 and Nod2. *J Biol Chem*. (2003) 278:41702–8. doi: 10.1074/jbc.M307198200
- Windheim M, Lang C, Peggie M, Plater LA, Cohen P. Molecular mechanisms involved in the regulation of cytokine production by muramyl dipeptide. *Biochem J*. (2007) 404:179–90. doi: 10.1042/BJ20061704
- Fritz JH, Girardin SE, Fitting C, Werts C, Mengin-Lecreux D, Caroff M, et al. Synergistic stimulation of human monocytes and dendritic cells by Toll-like receptor 4 and NOD1- and NOD2-activating agonists. *Eur J Immunol*. (2005) 35:2459–70. doi: 10.1002/(ISSN)1521-4141
- Shaw JM, Futch WS Jr., School LB. Induction of macrophage antitumor activity by acetylated low density lipoprotein containing lipophilic muramyl tripeptide. *Proc Natl Acad Sci U S A*. (1988) 85:6112–6. doi: 10.1073/pnas.85.16.6112
- Hoedemakers RM, Vossebeld PJ, Daemen T, Scherphof GL. Functional characteristics of the rat liver macrophage population after a single intravenous injection of liposome-encapsulated muramyl peptides. *J Immunother Emphasis Tumor Immunol*. (1993) 13:252–60. doi: 10.1097/00002371-199305000-00004
- Hedl M, Abraham C. NLRP1 and NLRP3 inflammasomes are essential for distinct outcomes of decreased cytokines but enhanced bacterial killing upon chronic Nod2 stimulation. *Am J Of Physiol Gastrointestinal And Liver Physiol*. (2013) 304:G583–96. doi: 10.1152/ajpgi.00297.2012
- Lessard AJ, LeBel M, Egarnes B, Prefontaine P, Theriault P, Droit A, et al. Triggering of NOD2 receptor converts inflammatory ly6C(high) into ly6C(low) monocytes with patrolling properties. *Cell Rep*. (2017) 20:1830–43. doi: 10.1016/j.celrep.2017.08.009
- Frampton JE. Mifamurtide: a review of its use in the treatment of osteosarcoma. *Paediatr Drugs*. (2010) 12:141–53. doi: 10.2165/11204910-000000000-00000
- Pashenkov MV, Dagil YA, Pinegin BV. NOD1 and NOD2: Molecular targets in prevention and treatment of infectious diseases. *Int Immunopharmacol*. (2018) 54:385–400. doi: 10.1016/j.intimp.2017.11.036
- Buteyn NJ, Santhanam R, Merchand-Reyes G, Murugesan RA, Dettorre GM, Byrd JC, et al. Activation of the intracellular pattern recognition receptor NOD2 promotes acute myeloid leukemia (AML) cell apoptosis and provides a survival

- advantage in an animal model of AML. *J Immunol.* (2020) 204:1988–97. doi: 10.4049/jimmunol.1900885
48. Nabergoj S, Mlinarič-Raščan I, Jakopin Ž. Harnessing the untapped potential of nucleotide-binding oligomerization domain ligands for cancer immunotherapy. *Medicinal Res Rev.* (2019) 39:1447–84. doi: 10.1002/med.21557
49. Shiny A, Regin B, Balachandhar V, Gokulakrishnan K, Mohan V, Babu S, et al. Convergence of innate immunity and insulin resistance as evidenced by increased nucleotide oligomerization domain (NOD) expression and signaling in monocytes from patients with type 2 diabetes. *Cytokine.* (2013) 64:564–70. doi: 10.1016/j.cyto.2013.08.003
50. Gavrillin MA, Bouakl JJ, Knatz NL, Duncan MD, Hall MW, Gunn JS, et al. Internalization and phagosome escape required for Francisella to induce human monocyte IL-1 β processing and release. *Proc Natl Acad Sci United States America.* (2006) 103:141–6. doi: 10.1073/pnas.0504271103
51. Merchand-Reyes G, Robledo-Avila FH, Buteyn NJ, Gautam S, Santhanam R, Fatehchand K, et al. CD31 acts as a checkpoint molecule and is modulated by fcgammaR-mediated signaling in monocytes. *J Immunol.* (2019) 203:3216–24. doi: 10.4049/jimmunol.1900059
52. Schindelin J, Arganda-Carreras I, Frise E, Kaynig V, Longair M, Pietzsch T, et al. Fiji: an open-source platform for biological-image analysis. *Nat Methods.* (2012) 9:676–82. doi: 10.1038/nmeth.2019
53. Shankar D, Merchand-Reyes G, Buteyn NJ, Santhanam R, Fang H, Kumar K, et al. Inhibition of BET proteins regulates fcgamma receptor function and reduces inflammation in rheumatoid arthritis. *Int J Mol Sci.* (2023) 24:1–14. doi: 10.3390/ijms24087623
54. McClanahan F, Riches JC, Miller S, Day WP, Kotsiou E, Neuberger D, et al. Mechanisms of PD-L1/PD-1-mediated CD8 T-cell dysfunction in the context of aging-related immune defects in the Emicro-TCL1 CLL mouse model. *Blood.* (2015) 126:212–21. doi: 10.1182/blood-2015-02-626754
55. Woyach JA, Bojnik E, Ruppert AS, Stefanovski MR, Goettl VM, Smucker KA, et al. Bruton's tyrosine kinase (BTK) function is important to the development and expansion of chronic lymphocytic leukemia (CLL). *Blood.* (2014) 123:1207–13. doi: 10.1182/blood-2013-07-515361
56. Merchand-Reyes G, Santhanam R, Robledo-Avila FH, Weigel C, Ruiz-Rosado JD, Mo X, et al. Disruption of nurse-like cell differentiation as a therapeutic strategy for chronic lymphocytic leukemia. *J Immunol.* (2022) 209:1212–23. doi: 10.4049/jimmunol.2100931
57. Veremeyko T, Yung AWY, Anthony DC, Strekalova T, Ponomarev ED. Early growth response gene-2 is essential for M1 and M2 macrophage activation and plasticity by modulation of the transcription factor CEBP β . *Front Immunol.* (2018) 9:2515. doi: 10.3389/fimmu.2018.02515
58. Jablonski KA, Amici SA, Webb LM, Ruiz-Rosado Jde D, Popovich PG, Partida-Sanchez S, et al. Novel markers to delineate murine M1 and M2 macrophages. *PLoS One.* (2015) 10:e0145342. doi: 10.1371/journal.pone.0145342
59. Zanello G, Goethel A, Forster K, Geddes K, Philpott DJ, Croitoru K. Nod2 activates NF- κ B in CD4+ T cells but its expression is dispensable for T cell-induced colitis. *PLoS One.* (2013) 8:e82623. doi: 10.1371/journal.pone.0082623
60. Wong KL, Tai JJ, Wong WC, Han H, Sem X, Yeap WH, et al. Gene expression profiling reveals the defining features of the classical, intermediate, and nonclassical human monocyte subsets. *Blood.* (2011) 118:e16–31. doi: 10.1182/blood-2010-12-326355
61. van Vugt MJ, Heijnen IAFM, Capel PJA, Park SY, Ra C, Saito T, et al. FcR γ -chain is essential for both surface expression and function of human fcyRI (CD64) *in vivo*. *Blood.* (1996) 87:3593–9. doi: 10.1182/blood.V87.9.3593.bloodjournal.8793593
62. Paolini R, Renard V, Vivier E, Ochiai K, Jouvin MH, Malissen B, et al. Different roles for the Fc epsilon RI gamma chain as a function of the receptor context. *J Exp Med.* (1995) 181:247–55. doi: 10.1084/jem.181.1.247
63. Ghalandary M, Li Y, Frohlich T, Magg T, Liu Y, Rohlf M, et al. Valosin-containing protein-regulated endoplasmic reticulum stress causes NOD2-dependent inflammatory responses. *Sci Rep.* (2022) 12:3906. doi: 10.1038/s41598-022-07804-1
64. Li S, Deng P, Wang M, Liu X, Jiang M, Jiang B, et al. IL-1 α and IL-1 β promote NOD2-induced immune responses by enhancing MAPK signaling. *Lab Invest.* (2019) 99:1321–34. doi: 10.1038/s41374-019-0252-7
65. Yang S, Wang B, Humphries F, Jackson R, Healy ME, Bergin R, et al. Pellino3 ubiquitinates RIP2 and mediates Nod2-induced signaling and protective effects in colitis. *Nat Immunol.* (2013) 14:927–36. doi: 10.1038/ni.2669
66. Bichi R, Shinton SA, Martin ES, Koval A, Calin GA, Cesari R, et al. Human chronic lymphocytic leukemia modeled in mouse by targeted TCL1 expression. *Proc Natl Acad Sci U S A.* (2002) 99:6955–60. doi: 10.1073/pnas.102181599
67. Herling M, Patel KA, Khalili J, Schlette E, Kobayashi R, Medeiros LJ, et al. TCL1 shows a regulated expression pattern in chronic lymphocytic leukemia that correlates with molecular subtypes and proliferative state. *Leukemia.* (2006) 20:280–5. doi: 10.1038/sj.leu.2404017
68. Hartmann TN, Grabovsky V, Wang W, Desch P, Rubenzer G, Wollner S, et al. Circulating B-cell chronic lymphocytic leukemia cells display impaired migration to lymph nodes and bone marrow. *Cancer Res.* (2009) 69:3121–30. doi: 10.1158/0008-5472.CAN-08-4136
69. Burgess M, Mapp S, Mazzieri R, Cheung C, Chambers L, Mattarollo SR, et al. Increased FcgammaRIIB dominance contributes to the emergence of resistance to therapeutic antibodies in chronic lymphocytic leukaemia patients. *Oncogene.* (2017) 36:2366–76. doi: 10.1038/onc.2016.387
70. Nimmerjahn F, Ravetch JV. Fcgamma receptors as regulators of immune responses. *Nat Rev Immunol.* (2008) 8:34–47. doi: 10.1038/nri2206
71. Minard-Colin V, Xiu Y, Poe JC, Horikawa M, Magro CM, Hamaguchi Y, et al. Lymphoma depletion during CD20 immunotherapy in mice is mediated by macrophage FcgammaRI, FcgammaRIII, and FcgammaRIV. *Blood.* (2008) 112:1205–13. doi: 10.1182/blood-2008-01-135160
72. Grandjean CL, Garcia Z, Lemaitre F, Breart B, Bousso P. Imaging the mechanisms of anti-CD20 therapy *in vivo* uncovers spatiotemporal bottlenecks in antibody-dependent phagocytosis. *Sci Adv.* (2021) 7:1–12. doi: 10.1126/sciadv.abd6167
73. Shehat MG, Cardona OA, Aranjuez GF, Jewett MW, Tigno-Aranjuez JT. RIP2 promotes FcgammaR-mediated reactive oxygen species production. *J Biol Chem.* (2019) 294:10365–78. doi: 10.1074/jbc.RA118.007218
74. Rosenzweig HL, Kawaguchi T, Martin TM, Planck SR, Davey MP, Rosenbaum JT. Nucleotide oligomerization domain-2 (NOD2)-induced uveitis: dependence on IFN- γ . *Invest Ophthalmol Vis Sci.* (2009) 50(4):1739–45. doi: 10.1167/iovs.08-2756
75. Kleinerman ES, Murray JL, Snyder JS, Cunningham JE, Fidler IJ. Activation of tumoricidal properties in monocytes from cancer patients following intravenous administration of liposomes containing muramyl tripeptide phosphatidylethanolamine. *Cancer Res.* (1989) 49:4665–70.
76. Kleinerman ES, Jia SF, Griffin J, Seibel NL, Benjamin RS, Jaffe N. Phase II study of liposomal muramyl tripeptide in osteosarcoma: the cytokine cascade and monocyte activation following administration. *J Clin Oncol Off J Am Soc Clin Oncol.* (1992) 10:1310–6. doi: 10.1200/JCO.1992.10.8.1310
77. Nardin A, Lefebvre ML, Labroquere K, Faure O, Abastado JP. Liposomal muramyl tripeptide phosphatidylethanolamine: Targeting and activating macrophages for adjuvant treatment of osteosarcoma. *Curr Cancer Drug Targets.* (2006) 6:123–33. doi: 10.2174/156800906776056473
78. Pahl JH, Kwappenberg KM, Varypataka EM, Santos SJ, Kuijper ML, Mohamed S, et al. Macrophages inhibit human osteosarcoma cell growth after activation with the bacterial cell wall derivative liposomal muramyl tripeptide in combination with interferon-gamma. *J Exp Clin Cancer Res Cr.* (2014) 33:27. doi: 10.1186/1756-9966-33-27
79. Dieter P, Hempel U, Kamionka S, Kolada A, Malessa B, Fitzke E, et al. Prostaglandin E2 affects differently the release of inflammatory mediators from resident macrophages by LPS and muramyl tripeptides. *Mediators Inflammation.* (1999) 8:295–303. doi: 10.1080/09629359990306
80. Ntoufa S, Vardi A, Papakonstantinou N, Anagnostopoulos A, Aleporou-Marinou V, Belessi C, et al. Distinct innate immunity pathways to activation and tolerance in subgroups of chronic lymphocytic leukemia with distinct immunoglobulin receptors. *Mol Med.* (2012) 18:1281–91. doi: 10.2119/molmed.2011.00480
81. Meyers PA, Schwartz CL, Krailo M, Kleinerman ES, Betcher D, Bernstein ML, et al. Osteosarcoma: a randomized, prospective trial of the addition of ifosfamide and/or muramyl tripeptide to cisplatin, doxorubicin, and high-dose methotrexate. *J Clin Oncol Off J Am Soc Clin Oncol.* (2005) 23:2004–11. doi: 10.1200/JCO.2005.06.031
82. Tacyildiz N, Unal E, Dincaslan H, Cakmak HM, Kose K, Tanyildiz G, et al. Muramyl tripeptide plus chemotherapy reduces metastasis in non-metastatic osteosarcoma: A single-center experience. *Asian Pacific J Cancer Prevention: APJCP.* (2020) 21:715–20. doi: 10.31557/APJCP.2020.21.3.715